Eur Biophys J (2011) 40:471–480
DOI 10.1007/s00249-010-0660-5

ORIGINAL PAPER

Interactions of a synthetic Leu–Lys-rich antimicrobial peptide with phospholipid bilayers

David I. Fernandez · Marc-Antoine Sani · John D. Gehman · Kyung-Soo Hahm · Frances Separovic

Received: 14 October 2010 / Revised: 4 December 2010 / Accepted: 14 December 2010 / Published online: 12 January 2011

Abstract The interaction of the synthetic antimicrobial peptide P5 (KWKKLLKKPLLKKLLKKL-NH_2) with model phospholipid membranes was studied using solid-state NMR and circular dichroism (CD) spectroscopy. P5 peptide had little secondary structure in buffer, but addition of large unilamellar vesicles (LUV) composed of dimyristoylphosphatidylcholine (DMPC) increased the β-sheet content to ~20%. Addition of negatively charged LUV, DMPC–dimyristoylphosphatidylglycerol (DMPG) 2:1, led to a substantial (~40%) increase of the α-helical conformation. The peptide structure did not change significantly above and below the phospholipid phase transition temperature. P5 peptide interacted differently with DMPC bilayers with deuterated acyl chains (d_{54}-DMPC) and mixed d_{54}-DMPC–DMPG bilayers, used to mimic eukaryotic and prokaryotic membranes, respectively. In DMPC vesicles, P5 peptide had no significant interaction apart from slightly perturbing the upper region of the lipid acyl chain with minimum effect at the terminal methyl groups. By contrast, in the DMPC–DMPG vesicles the peptide increased disorder throughout the entire acyl chain of DMPC in the mixed bilayer. P5 promoted disordering of the headgroup of neutral membranes, observed by ^{31}P NMR. However, no perturbations in the T_1 relaxation nor the T_2- values were observed at 30°C, although a slight change in the dynamics of the headgroup at 20°C was noticeable compared with peptide-free vesicles. However, the P5 peptide caused similar perturbations of the headgroup of negatively charged vesicles at both temperatures. These data correlate with the non-haemolytic activity of the P5 peptide against red blood cells (neutral membranes) while inhibiting bacterial growth (negatively charged membranes).

Keywords Antimicrobial peptide · Model membranes · Peptide-lipid interaction · Circular dichroism · Solid-state NMR

D. I. Fernandez and M.-A. Sani contributed equally to the publication.

Membrane-active peptides: 455th WE-Heraeus-Seminar and AMP 2010 Workshop.

D. I. Fernandez · M.-A. Sani · J. D. Gehman · F. Separovic (✉)
School of Chemistry, Bio21 Institute,
University of Melbourne, Melbourne, VIC 3010, Australia
e-mail: fs@unimelb.edu.au

K.-S. Hahm
Research Centre for Proteineous Materials (RCPM),
Chosun University, 375 Seosuk-Dong, Dong-Ku,
Gwangju, Republic of Korea

Introduction

Current and previous generations of antibiotics have typically been active against structural and enzymatic targets unique to bacteria (Bycroft and Shute 1985, Shakil et al. 2008, Hooper 2001, Oliphant and Green 2002). As the number of bacteria resistant to multiple current antibiotics increases, research is in progress to develop new antimicrobial compounds which identify and exploit other differences between eukaryotic and prokaryotic cells. Marked differences between the phospholipid content of prokaryotic and eukaryotic membranes (Epand et al. 2006) are one possibility whereby an emerging group of promising molecules, antimicrobial peptides, preferentially interact with and disrupt the integrity of microbial membranes.

Antimicrobial peptides are generally small (6–50 amino acids), amphipathic molecules with different lengths,

sequences, and structures (Guiliani et al. 2007). These molecules have activity against a range of microorganisms, for example bacteria, protozoa, yeasts, fungi, and, occasionally, tumours. It has been shown that antimicrobial peptides usually act via non-receptor-mediated mechanisms which result in the disruption of membranes, with evidence suggesting that the membrane bilayer phospholipid composition is an important determinant of peptide activity (Fernandez et al. 2009). Two general mechanisms for these membrane-disruptive peptides have been proposed (Oren and Shai 1999, Shai 1999). The peptides may bind to the membrane surface, making the structure permeable, in a detergent like manner, or insert either partially or fully into the membrane causing pore formation or membrane disruption (Oren and Shai 1999, Shai 1999, Shai and Oren 2001, Yang et al. 2001).

P5 peptide (KWKKLLKKPLLKKLLKKL-NH_2) is a synthetic antimicrobial peptide the design of which was inspired by the structures of cecropin A and magainin 2 (Park et al. 2003, 2006). In a previous study, a hybrid peptide composed of the N-terminal amphipathic region of cecropin A (1–8) and the hydrophobic region of magainin 2 (1–12) had more antimicrobial activity than the native peptides (Park et al. 2003). Several further analogues were designed by increasing the net positive charge and hydrophobicity through extensive Leu and Lys substitution and flexible hinge replacement (Gly–Ile–Gly → Pro). The most active analogue, "P5", with net charge +9, was chosen for further study. P5 peptide has been found to be broad-acting (Table 1), being active against numerous Gram-positive and negative bacteria, for example *S. aureus, B. subtilis, S. epidermis, P. aeruginosa, P. vulgaris*, and *S. typhimurium,* as well as anti-fungal (*C. albicans, T. beigelii*) and anti-tumour activity (Park et al. 2003, 2006). Significantly, despite the broad range of activity, P5 peptide is not haemolytic below 100 μM, making it a potential candidate for future therapeutic use in humans.

Table 1 Minimum inhibitory and minimum bactericidal concentrations of P5 peptide

Organism	MIC (μM)	MBC (μM)
S. aureus	1.56	3.13
B. subtillis	0.78	1.56
S. epidermis	3.13	3.13
P. vulgaris	1.56	3.13
P. aeruginosa	1.56	1.56
S. typhimurium	0.09	0.09
C. albicans	6.25	–
T. beigelii	3.25	–

Park et al. (2003, 2006)

Previous studies have reported that P5 peptide interacts with bacterial membranes, leading to depolarisation and permeabilisation, while inducing observable cell surface defects in a similar manner to the strongly haemolytic melittin (Park et al. 2003, 2006). In an effort to obtain more information about the mechanism of action of this peptide, solid-state NMR and circular dichroism (CD) studies were conducted using model membrane systems chosen to mimic the essential charge characteristics of mammalian and bacterial membranes. Mammalian membranes contain neutral and negatively charged phospholipids but the negatively charged phospholipids are located mainly in the inner layer with the exposed outer layer containing phospholipids with neutral or zwitterionic lipid headgroups (Cornell and Separovic 1983). Bacterial membranes, in contrast, contain more lipids with anionic headgroups, providing an overall net negative charge. The secondary structure adopted by P5 peptide in neutral and anionic membrane environments, and the effect of the peptide on phospholipid bilayer structure and dynamics are reported below.

Materials and methods

Preparation of phospholipid NMR samples

Perdeuterated-acyl chain dimyristoylphosphatidylcholine (d_{54}-DMPC) and natural abundance dimyristoylphosphatidylglycerol (DMPG) were purchased from Avanti Polar Lipids (Alabaster, AL, USA), and used without further purification. Pure d_{54}-DMPC and mixed d_{54}-DMPC–DMPG (2:1 molar ratio) lipid systems were prepared and P5 peptide added at 30:1 lipid-to-peptide (L/P) molar ratio. Phospholipids were dissolved in chloroform–methanol (9:1) and a rotary evaporator was used to form a thin film before samples were placed under a high vacuum overnight to remove trace amounts of solvent.

Dried lipid thin films were hydrated with 10× the lipid mass of 1 mM MOPS buffer (3-(*N*-morpholino)propanesulfonic acid) before being lyophilised. The dried samples were re-hydrated with 1× the lipid mass of Milli-Q water to prepare a 50% (*w*/*w*) hydrated sample in 10 mM MOPS buffer (pH 7.3) and subjected to five freeze–thaw cycles before being transferred to NMR rotors.

Preparation of peptide–lipid NMR samples

P5 peptide (KWKKLLKKPLLKKLLKKL-NH_2) of purity >98% was obtained from AnyGen (Gwangju, Korea) and the Bio21 peptide facility (Melbourne, Australia). To remove any trifluoroacetic acid remaining from the purification procedure, HCl solution was added before lyophilization (Sani et al. 2007). Peptide was solubilised in 10× the

lipid mass of 1 mM MOPS buffer and used to hydrate dried lipid mixtures to a final 30:1 L/P molar ratio. Samples were lyophilised and hydrated as described above for the lipid only systems. Typically 1 mg peptide and 10 mg phospholipid were used.

Solid-state NMR experiments

Static deuterium spectra were obtained at 46.09 MHz on a Varian (Palo Alto, CA, USA) Inova-300 spectrometer by using a composite pulse solid echo sequence. The operating conditions included 4.1-μs 90° pulses, 40 μs echo delay, and 0.5 s recycle delay. Spectra were collected with a 2-μs dwell time but with 70 kHz audio filter bandwidth and optimised incomplete final echo delay (Lau et al. 2007) such that left-shifting enabled Fourier transformation at the top of the echo. This results in optimised lineshape with zero frequency-dependent phase correction (Davis 1983). A minimum of 28 k scans were collected and Fourier transformed using zero-filling to 2^{14} points, 200 Hz Gaussian line broadening, and zero-order phase correction only to generate unoriented powder spectra. Oriented spectra were generated by numerically "de-Paking" with the single value decomposition method (Whittall 1989), using utilities in the GNU Scientific Library (Galassi et al. 2009). Gaussian lineshapes with uniform linewidths and intensities (except for slightly narrowed and 50% more intense CD_3) were fit to the de-Paked spectrum and converted to order parameters by dividing the symmetric splitting for each of 26 myristoyl-CD positions by the static coupling constant of 255 kHz (Davis et al. 1980). The quality of the de-Paked spectra and of the Gaussian approximations was confirmed by "re-Paking", and comparing with the original raw spectral data.

^{31}P static and magic-angle spinning (MAS) solid-state NMR experiments were performed at 242.76 MHz on a Varian 600-MHz spectrometer using a 3.2 mm HXY BioMAS probe (Varian). Static ^{31}P NMR spectra were collected under SPINAL proton decoupling (Fung et al. 2000) using a single $\pi/2$-pulse with a duration of 4.4 μs. A minimum of 1,024 transients were averaged at a spectral width of 125 kHz, and were Fourier transformed after 100-Hz exponential line broadening. ^{31}P relaxation experiments were carried out under MAS at 4 kHz. T_1 relaxation times were measured using the inversion recovery pulse sequence (Cornell et al. 1983). Typical recycle delays were 4 s with variable τ-delay values between 0 and 4 s. T_2 relaxation times were measured with a Hahn spin–echo experiment with total echo delay (τ) values between 0.5 and 30 ms using integer multiples of the rotor period. Relaxation times were calculated using non-linear curve fits of both the intensities and integrals of peaks versus τ using Origin Pro 8. Relaxation curve fitting using integrals compared favourably with fits from peak heights.

Static ^{31}P NMR spectra were analysed by straightforward deconvolution of data into a user-specified number of asymmetric, axially symmetric, and/or isotropic components. One-hundred and eighty angles between 0 and $\pi/2$ were used (for all relevant orientation angles) with a 60% Gaussian and 40% Lorentzian lineshape centred on the appropriate frequency, and weighted according to the statistical probability of the angles. Chemical shifts, angle-dependent linewidths (Seelig 1978), and fraction of each component were optimized by scaled Levenberg–Marquardt (Mor'e 1978) nonlinear fitting routines in the Gnu Scientific Library (Galassi et al. 2009). Algorithm performance was tested against data simulated in Simpson (Bak et al. 2000).

Preparation of circular dichroism samples

DMPC and mixed DMPC–DMPG (2:1) dry lipid thin films were hydrated with Milli-Q water (typically 0.5 ml/10 mg lipid) before being lyophilised. The dried samples were hydrated with 10 mM MOPS buffer to produce a final concentration of 5 mM phospholipid and subjected to several freeze–thaw steps before being extruded above 25°C through 100 nm polycarbonate membranes to produce large unilamellar vesicles (LUV). Immediately before CD measurements, phospholipid LUVs were diluted with additional 10 mM MOPS buffer and P5 peptide to produce solutions of 1:10, 1:30, 1:50, and 1:100 lipid-to-peptide ratio. The peptide concentration was kept at 30 μM.

Circular dichroism experiments

Circular dichroism spectra were acquired on a Jasco (USA) J-815 spectropolarimeter. Spectra of peptide solutions were recorded between 190 and 250 nm using a 1 mm pathlength quartz cell (Starna, Australia). Samples were left to equilibrate for 5 min at 30°C before accumulation of three scans. The lipid background was subtracted. To estimate the peptide secondary structure content, analysis of the relevant CD spectra was carried out using CDPro software (http://lamar.colstate.edu/~ssreeram/CDPro) developed by Woody and co-workers (Sreerama and Woody 1993). CD values were converted to mean residue ellipticity (MRE). Basis set 7 of the CDPro software was used and analysis was performed using three methods, CONTIN, CONTIN/LL and SELCON 3 (Sreerama and Woody 2000, 2004). In general, CONTIN/LL, a self-consistent method with an incorporated variable selection procedure, produced the most reliable results.

Results

Circular dichroism was conducted on P5 peptide with phospholipid suspensions of DMPC and DMPC–DMPG (2:1) to investigate the secondary structure adopted by this peptide in membrane mimetic environments. ^{31}P and ^{2}H solid-state NMR techniques were used to investigate the interaction between P5 peptide and phospholipid bilayer membranes. These studies probed changes in phospholipid motion and conformation over a range of time scales.

Secondary structure of P5 peptide by circular dichroism

The membrane mediated conformational change of P5 was characterized by use of CD spectra in the 250–190 nm range. CD spectra were acquired at 30°C to ensure that the lipids were above the fluid phase transition temperatures of 23°C for DMPC and DMPG (Silvius 1982). The CD spectra of P5 before and after addition of LUV of different surface charge are shown in Fig. 1. In the absence of vesicles, the spectrum of the membrane-free peptide contained a broad single minimum at approximately 197 nm, indicating a dominant unstructured conformation. Deconvolution using a protein structure data set confirmed 90% of random coil structures (Table 2). Addition of LUV composed of DMPC did not trigger any major conformation change except at high L/P ratio where a weak decrease of the minimum was observed (Fig. 1 bottom panel). This is likely to be because of light scattering in the low-wavelength region. However, the increase in β-sheet at high L/P ratio (Table 2) may be because of aggregation of the peptide with DMPC. No significative difference was observed between experiments at 30 or 20°C. Interestingly, adding LUV composed of DMPC–DMPG (2:1) induced significant changes in the P5 CD spectra (Fig. 1 top panel). Indeed, the negatively charged vesicles promoted typical features of helical conformation with two minima at 222 and 208 nm and a broad maximum around 195 nm. From L/P 30:1–100:1, approximately 40% of α-helix was obtained after deconvolution (Table 2).

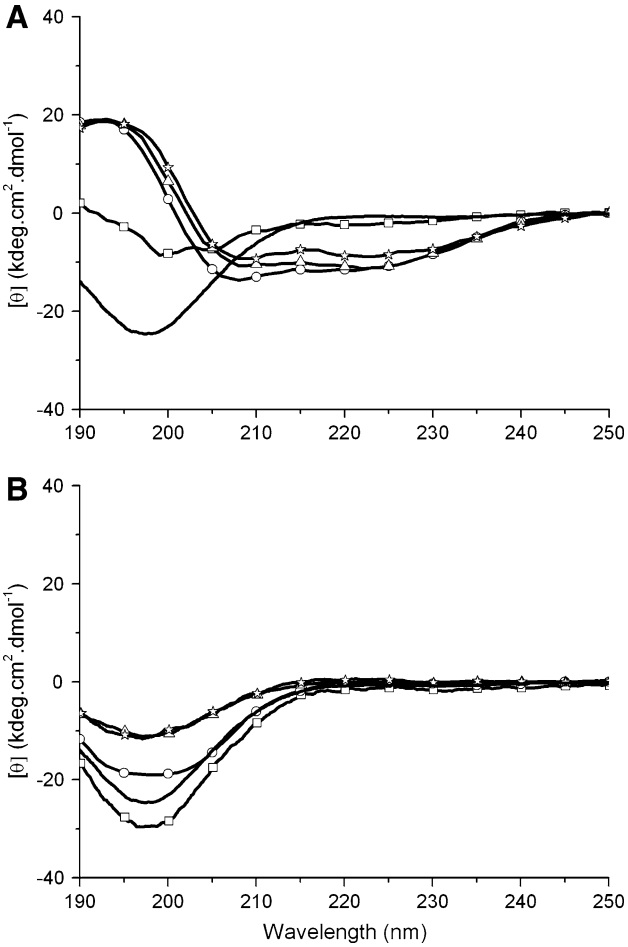

Fig. 1 CD spectra of P5 peptide on addition of LUV composed of DMPC (*bottom panel*) or DMPC–DMPG 2:1 molar ratio (*top panel*). Lipid-to-peptide molar ratio, L/P: 10:1 (*squares*), 30:1 (*circles*), 50:1 (*triangles*), and 100:1 (*stars*). Three scans were accumulated at 30°C

Acyl chain interaction with P5 peptide using ^{2}H static solid-state NMR

^{2}H NMR spectra of a deuterium-labelled phospholipid bilayer provide a sensitive probe for determining the order and range of motions undergone by the lipid acyl chains. The static deuterium spectrum of a perdeuterated acyl chain yields a complex line shape (Pake powder pattern) for each individual deuterated position. Alterations in the splittings (width) of the powder pattern provide an indication of changes in acyl chain order or packing, with an increase indicating increased order and vice versa. ^{2}H NMR experiments were performed to determine if the P5 peptide perturbed the phospholipid acyl chains. All ^{2}H NMR spectra were de-Paked by use of in-house software (Materials and methods section) and order parameter profiles were generated. An example of the experimental data and the re-Paked spectra of the peptide-free DMPC–DMPG mixture is displayed in Fig. 2, upper panel, and the de-Paked spectra, and the Gaussian approximation used, are displayed in Fig. 2, lower panel.

At 30°C, the DMPC control sample had a typical fluid-phase order parameter profile, with rigidity decreasing from the upper acyl chain region to the terminal methyl region, whereas including DMPG produced an ordering effect among the acyl chains in the interior of the bilayer (Fig. 3, solid symbols). In the presence of P5 peptide (Fig. 3, open symbols), the order parameters of the C–D bonds close to the glycerol backbone decreased by ~5% relative to pure d_{54}-DMPC, indicating that peptide addition increased disorder in the upper acyl chain region of the bilayer. The

Table 2 CD analysis of P5 peptide in DMPC and DMPC–DMPG LUVs

Secondary structure (%) of the P5 peptide[a] on titration with DMPC or DMPC–DMPG LUV[b]					
	L/P molar ratio	α-Helix[c]	β-Sheet[c]	Turn[c]	Random coil[c]
MOPS buffer		2	4	4	90
DMPC	10	3	1	3	93
	30	3	12	9	76
	50	2	21	10	67
	100	2	25	12	61
DMPC–DMPG 2:1	10	5	28	13	54
	30	41	10	19	30
	50	38	13	19	30
	100	40	14	17	29

[a] Peptide concentration fixed at 30 μM, experiment conducted at 30°C (no significant change at 20°C)

[b] Large unilamellar vesicle of 100 nm diameter

[c] Deconvolution of CD spectra was accomplished using basis 7 from CDPro software (Sreerama and Woody 2000) and the CONTIN/LL algorithm

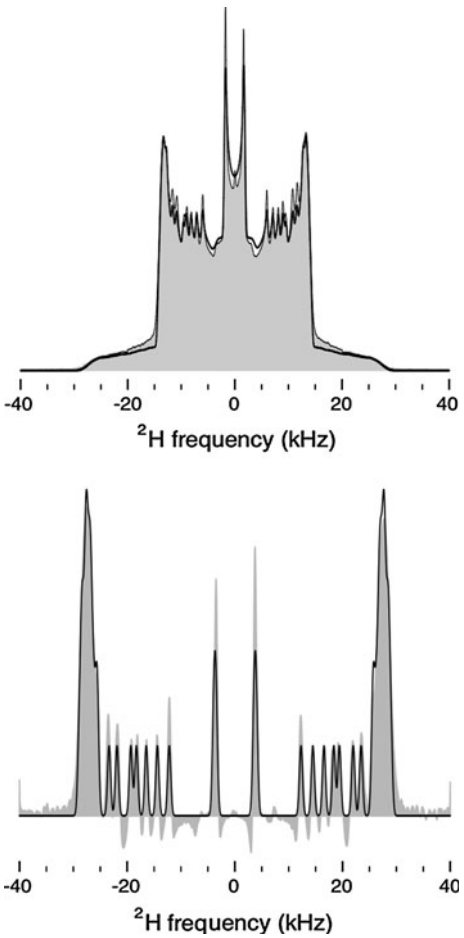

Fig. 2 *Upper panel* ^{2}H NMR experimental spectrum of d_{54}-DMPC–DMPG (2:1 molar ratio) (*fill*) at 30°C, where the "re-Paked" solution is overlayed (*thin line*) on the "re-Paked" solution to the Gaussian approximation (*thick line*). *Lower panel* de-Paked spectrum (*grey fill*) of d_{54}-DMPC–DMPG (2:1 molar ratio) superimposed on the 26-Gaussian fit (*solid line*)

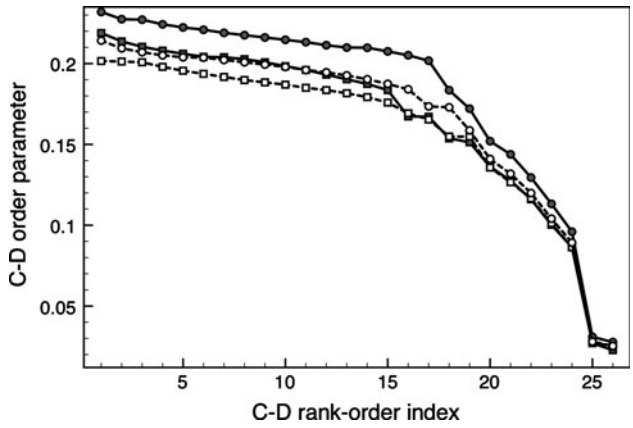

Fig. 3 Order parameter profile obtained from de-Paked spectra of d_{54}-DMPC (*solid squares*), d_{54}-DMPC–DMPG at 2:1 molar ratio (*solid circles*), and with addition of P5 peptide at an L/P ratio of 30:1 (*open symbols*). Experiments performed at 30°C

terminal methyl order parameter did not change significantly, suggesting that the interior of the bilayer was not perturbed. In the anionic mixed d_{54}-DMPC–DMPG system, addition of P5 peptide resulted in an order parameter decrease of approximately 10% at all DMPC chain positions. This suggests that the peptide penetrates deeper into the hydrophobic core of the bilayer. Moreover, the d_{54}-DMPC in the mixed PC–PG bilayer with P5 had splittings similar to pure DMPC bilayers, suggesting that the peptide could segregate DMPG by preferential interaction.

Probing headgroup region and lipid dynamics by static and MAS ^{31}P solid-state NMR

The ^{31}P spectrum of a phospholipid bilayer provides information about the local order and conformation of the

phosphate region of the headgroup (Seelig 1978), and about the lipid phase (Cullis and de Kruijff 1979). Static ^{31}P NMR of unoriented phospholipid liposomes in the liquid-lamellar phase, because of the fast axial reorientation of the lipid molecules, results in an axially symmetric CSA with an overall width that depends on ^{31}P headgroup orientation and disorder (Seelig 1978). The static ^{31}P line shape is used to probe perturbations to headgroup orientation and dynamics on the 10^{-4} s timescale. The ^{31}P spectra of DMPC and mixed DMPC–DMPG multilayers at 30°C are shown in Fig. 4. The ^{31}P spectrum of DMPC has a typical axially symmetric powder pattern with a CSA of ~46 ppm in the fluid phase (above 25°C) whereas a broader lineshape was observed at 20°C, with a CSA characteristic of a gel phase of approximately 55 ppm (Table 3). For the mixed lipids, the ^{31}P CSA is a combination of both DMPC and DMPG with CSA of 42 and 32 ppm, respectively, as extracted from deconvolution (Fig. 4, top rows). This indicated that the presence of DMPG slightly disorders the headgroup region or enables the headgroups to bend away from the bilayer normal. Cooling the sample below the fluid phase transition resulted in a CSA increase to 49 ppm where the PC and PG CSAs were no longer distinct (spectra not shown). The P5 peptide had a somewhat similar effect on both vesicle compositions, as an overall CSA reduction, at 20 or 30°C, indicating that the peptide was disordering and/or altering the orientation of the phospholipid headgroups. However, P5 caused a lesser decrease in the mixed anionic DMPC–DMPG bilayers (3–5 ppm) compared with the resulting effect on the neutral bilayers (5–14 ppm) as observed in Fig. 4, bottom row, and Table 3.

To observe the effect of the peptide on each lipid component individually, high-resolution MAS experiments were performed in which DMPC and DMPG phosphate signals can be observed at their different isotropic chemical shifts (σ_i). At 8 kHz MAS speed, the CSA for the phospholipids are entirely averaged out and intensity from all orientations is averaged into a narrow peak as observed in Fig. 5. The ^{31}P MAS spectra of DMPC multilayers with and without peptide gave a single peak at −1.0 ppm at both 30 or 20°C (Fig. 5b). MAS spectra of DMPC–DMPG vesicles revealed two resonances at −0.9 and +0.2 ppm. Deconvolution revealed at 3:1 molar ratio for peptide-free DMPC–DMPG vesicles, somewhat different from the P5-containing DMPC–DMPG sample for which a 2:1 molar ratio was calculated (not shown). P5 peptide promoted a significant upfield shift by 0.2 ppm on both resonances (Fig. 5a; top spectra). Again, no significant change was observed between 30 or 20°C except overall broadening due to slower tumbling dynamics, as reported in the relaxation measurements.

^{31}P relaxation studies: Measurement of T_1 and T_2 relaxation times are used to characterise intensities of fluctuations on different timescales. After application of a radio-frequency pulse, excited nuclei relax to thermal equilibrium through different mechanisms such as T_1 and T_2 relaxation. In the context of the T_1 and T_2 relaxation rates of the ^{31}P nuclei in lipid bilayer headgroups, T_1 reports primarily on individual lipid dynamics on the nanosecond timescale (Separovic et al. 2000) whereas T_2 reports on slower collective membrane motions on the millisecond and slower timescale (Cornell et al. 1982; 1983). These relaxation times may

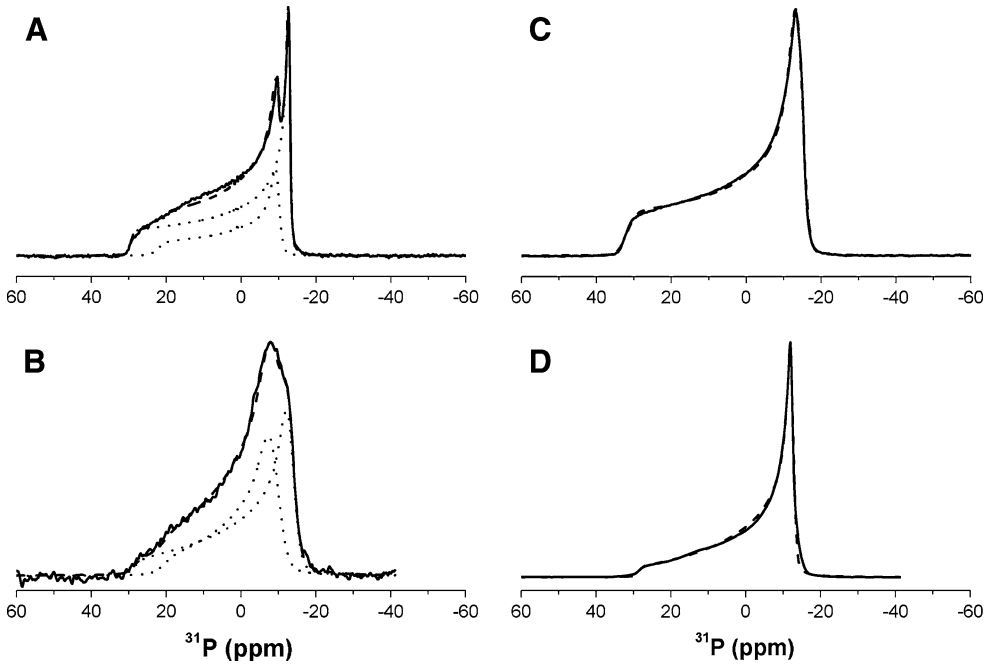

Fig. 4 Deconvolution of static ^{31}P NMR spectra. DMPC–DMPG (2:1) multilayers without, **a**, and with, **b**, P5 peptide (30:1); and DMPC multilayers without, **c**, and with, **d**, P5 peptide (30:1). The *dashed lines* are the sum of the deconvoluted components (*dotted lines*); the *unbroken lines* are the experimental spectra obtained at 30°C

Table 3 ^{31}P NMR CSA and relaxation times

	DMPC	DMPC + P5 (30:1)	PC–PG[a] (2:1)	PC–PG + P5 (20:10:1)
^{31}P Chemical shift anisotropy[b]				
^{31}P CSA (ppm) at 30°C	46	41	42/32	42/29
^{31}P CSA (ppm) at 20°C	55	41	49	45
^{31}P relaxation times[c]				
T_1 (s) at 30°C	0.66	0.65	0.46/0.32	0.23/0.18
T_2 (ms) at 30°C	12.7	12.8	7.9/4.3	2.0/1.6
T_1 (s) at 20°C	0.65	0.77	0.4	0.16
T_2 (ms) at 20°C	0.79	0.62	0.68	0.4

[a] The two values obtained at 30°C represent those from a DMPC and DMPG-enriched phase

[b] CSA extracted from deconvolution of static ^{31}P NMR spectra by use of in-house software (J.D. Gehman; Materials and methods section)

[c] T_1 and T_2 experiments were performed at 4 kHz spinning speed; exponential decay functions were used to fit intensities of isotropic centre resonances (Materials and methods section)

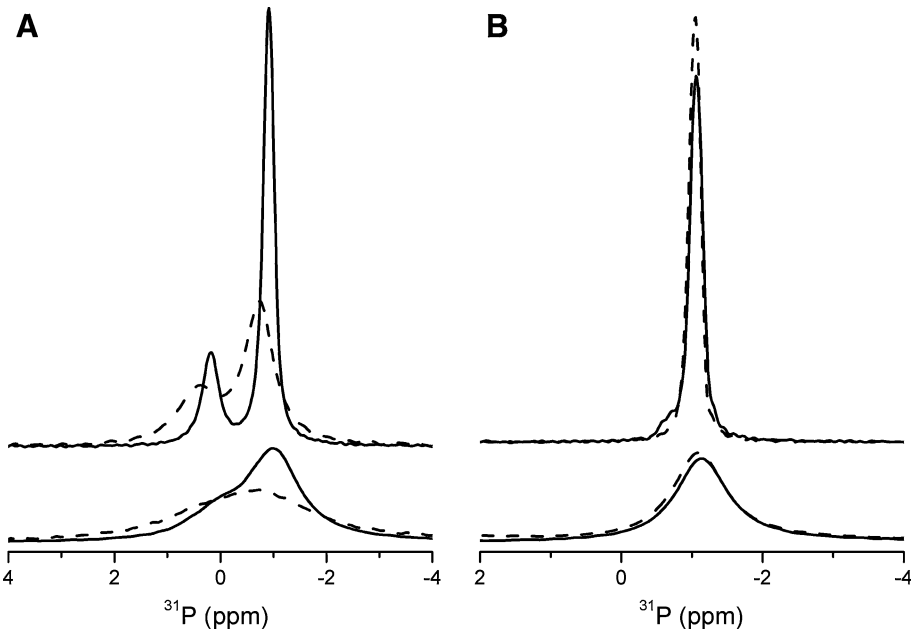

Fig. 5 ^{31}P MAS NMR spectra of **a** DMPC–DMPG (2:1) multilayers without (*unbroken line*) and with (*dashed line*) P5 peptide (30:1), and **b** DMPC multilayers without (*unbroken line*), and with (*dashed line*) P5 peptide (30:1). The upper spectra were obtained at 30°C and the lower spectra at 20°C under 8 kHz MAS

be used to assist in identifying changes in molecular motion, for example those induced by the presence of added molecules such as peptides.

Table 3 summarises the ^{31}P T_1 and T_2 relaxation times for the relaxation measurements of each lipid system at 4 kHz MAS. For the pure DMPC lipid system at 30°C, the T_1 and T_2 relaxation times were ~0.66 s and ~12.7 ms, respectively. Reducing the temperature to 20°C had a minimal effect on T_1 relaxation times, but reduced the T_2 relaxation time substantially, to 0.79 ms, suggesting no significant change in the intensity of the dynamics of individual phospholipids but increased global bilayer motion. Likewise, addition of P5 peptide to the DMPC system at 30°C caused no significant observable change in headgroup relaxation dynamics, suggesting that P5 peptide has little or no persistent interaction with the surface of the bilayer. A similar effect was observed at 20°C.

The presence of DMPG increased the dynamics experienced by the DMPC headgroup, with a reduction in both T_1 and T_2 from 0.66 to 0.46 s and 12.7 to 7.9 ms, respectively. This indicated that, as for the static ^{31}P spectra, addition of DMPG slightly disordered the headgroup region or enabled the headgroups to change orientation away from the bilayer normal. Under 4 kHz MAS, sufficient resolution was achieved to resolve both the DMPC and DMPG components contributing to the spectrum. At 30°C, the DMPC component produced a T_1 and T_2 of 0.46 s and 7.9 ms respectively, whereas the DMPG component gave a T_1 of

0.32 s and a T_2 of 4.3 ms. After addition of P5 peptide, both DMPC and DMPG experienced a ~50% reduction in T_1 relaxation time whereas T_2 values were reduced by ~75% for DMPC and ~65% for DMPG. This significant decrease in both relaxation times indicates that P5 peptide increases the dynamics experienced by the phospholipid headgroups on both the fast (ns) and slow (ms) timescales. The decrease in T_1 probably indicates an increase in the magnitude of motions of individual lipid headgroups. Similarly, the decrease in T_2 indicates an increased intensity of low-frequency fluctuations in the local magnetic environment about the ^{31}P nuclei and may correspond to increases in collective bilayer surface motion or direct perturbation of the local magnetic environment of the headgroups by the peptide.

Discussion

The broad range of antimicrobial activity of the synthetically designed P5 peptide (Table 1) with a lack of observed haemolysis of red blood cells (Park et al. 2006) renders it an attractive candidate for future therapeutic use. Previous studies using confocal microscopy with fluorescently labelled peptide revealed that on addition to fungi P5 peptide penetrates the cell wall before accumulating within the plasma membrane (Park et al. 2003). Similarly, propidium iodide permeabilisation studies on the effect of P5 peptide on *S. aureus* and measurement of the transmembrane potential revealed permeabilisation of the bacterial cell membrane and membrane depolarisation (Park et al. 2006). In a similar manner, scanning electron microscopy has shown that P5 peptide induces significant disruption of the cell surface structure of *S. aureus* and *P. aeruginosa*, in a manner similar to that of melittin (Park et al. 2003, 2006). However, unlike melittin, P5 is not strongly haemolytic and in that respect is more like cecropin A and magainin. These results and the broad range of activity of P5 peptide (Table 1) indicate that the likely mechanism of action involves direct interaction with, and disruption of, the membrane structure of microorganisms, which may proceed via one of the general mechanisms mentioned previously (Oren and Shai 1999).

Because the bacterial membrane is a principal determinant of biological activity, it is important to further investigate these interactions using systems that capture the essential characteristics without introducing undue complexity. Differences in membrane composition have long been thought to be important in the selectivity of antimicrobial peptides. In this study it was shown that inclusion of an anionic phospholipid in an otherwise net-neutral membrane system enabled selective interaction with the cationic P5 peptide.

P5 peptide in DMPC membranes

The weak perturbation of the bilayers in the fluid phase, in combination with a lack of secondary structure detected by CD, suggests that this peptide is inactive toward membranes with the charge and fluidity characteristics of eukaryotic organisms; an observation that correlates strongly with recorded activity data (Table 1) and lack of haemolytic activity toward red blood cells (Park et al. 2003). Although previous studies have shown that the effects of P5 peptide on the cell surface of bacteria are similar to those of melittin, the absence of any significant interaction with neutral membranes suggests P5 operates via a different mode of action. Indeed, deuterium NMR revealed that addition of P5 peptide to DMPC (model eukaryotic) bilayers resulted in disordering of the C–D bonds nearest the membrane surface only, while having a minimal effect on the end of the acyl chain at the centre of the bilayer. Furthermore, no isotropic phase was apparent in the static ^{31}P spectra, indicating that although the peptide disturbed the surface of the membrane, as observed in the ^{31}P CSA reduction (Table 3), overall bilayer integrity was preserved, even in the gel phase in which antimicrobial peptides have been seen to promote bilayer disruptions (Bechinger 2005), possibly because of peptide intercalation at domain defects. ^{31}P NMR relaxation times of this system revealed that, compared with pure DMPC bilayers, P5 peptide did not cause any observable alteration in T_1 and T_2 relaxation times at 30°C but had a more substantial effect on the headgroup dynamics of DMPC bilayers at 20°C. The effects observed at 20°C are most likely to be because a portion of the peptide is trapped between multilamellar vesicle bilayers with restricted motion freedom. This supports a peripheral and unspecific interaction with DMPC phospholipids compared with anionic bilayers, as discussed below.

P5 peptide in DMPC–DMPG membranes

The electrostatic interaction between P5 peptides and the (anionic) model prokaryotic bilayers resulted in a clear conformational change toward helical structures (~40%). The strong interaction promoted a disordering effect on the deuterated acyl chains of DMPC, from the headgroup region and extending further into the centre of the bilayer (Fig. 3) The static ^{31}P NMR spectrum revealed minimal effects on bilayer headgroup orientation apart from a minor narrowing of the CSA of the anionic DMPG lipids, which may ensue from primarily electrostatic recognition of the negatively charged membrane (Table 3).

Although the peptide seemed to interact with the acyl chains of the deuterated DMPC, these interactions may be peripheral, because the cationic P5 peptide is likely to interact primarily with the negatively charged DMPG lipids.

Together with evidence of significant bilayer headgroup interaction, if P5 peptide preferentially interacts with the DMPG, any effects on the acyl chains of DMPC will be largely indirect, and more direct effects will be noted on the PG headgroup. Perturbation of the DMPC acyl chains and the similar 50% reduction in headgroup relaxation time and the overall downfield isotropic chemical shift suggests that interaction of P5 peptide has an effect on the entirety of the bilayer. Thus, P5 is likely to penetrate much further into the acyl chain interior of the net anionic membrane. Only the ^{31}P CSA of PG lipids in the mixed PC–PG bilayers at 30°C seems to be reduced, which suggests P5 partially partitions into the bilayer and has more of a disordering effect on a DMPG-enriched bilayer because of electrostatic affinity. This is confirmed by the increased reduction of the ^{31}P CSA at 20°C, at which temperature the peptide may be less well-accommodated in a more rigid acyl chain environment as encountered in the gel phase, which could increase the peripheral peptide population.

Conclusion

These solid-state NMR results for P5 peptide in model membranes indicate that this synthetic peptide resides primarily near the surface of model eukaryotic bilayers and exists in an unstructured form without significantly interacting with the bilayer. Previous activity studies (Park et al. 2003, 2006) suggest P5 has minimal effects on red blood cells. By contrast, in model prokaryotic (anionic) bilayers, P5 peptide rearranges into an α-helix, significantly increasing headgroup dynamics, while also seeming to penetrate further into the membrane. These results are consistent with P5 peptide aggregating on the surface of neutral bilayers with minimal effect on the host organism, while adopting an orientation that penetrates and enters the acyl chain interior of anionic bilayers. Given the propensity of prokaryotic organisms to contain membranes with higher anionic phospholipid content, it is likely that this peptide exerts its antimicrobial activity by disruption of the membrane bilayer.

Acknowledgments DIF is the recipient of an Australian Postgraduate Award. JDG is the recipient of an Australian Research Council Future Fellowship (FT0991558).

References

Bak M, Rasmussen JT, Nielsen NC (2000) Simpson: a General simulation program for solid-state NMR spectroscopy. J Magn Reson 147:296–330

Bechinger B (2005) Detergent-like properties of magainin antibiotic peptides: a ^{31}P solid-state NMR spectroscopy study. Biochim Biophys Acta 1712:101–108

Bycroft BW, Shute RE (1985) The molecular basis for the mode of action of beta-lactam antibiotics and mechanisms of resistance. Pharm Res 2(1):3–14

Cornell BA, Separovic F (1983) Membrane thickness and acyl chain length. Biochim Biophys Acta 733:189–193

Cornell BA, Davenport JB, Separovic F (1982) Low frequency motion in membranes: the effect of cholesterol and proteins. Biochim Biophys Acta 689:337–345

Cornell BA, Hiller RG, Raison J, Separovic F, Smith R, Vary JC, Morris C (1983) Biological membranes are rich in low frequency motion. Biochim Biophys Acta 732:473–478

Cullis PR, de Kruijff B (1979) Lipid polymorphism and the functional roles of lipids in biological membranes. Biochim Biophys Acta 559:399–420

Davis JH (1983) The description of membrane lipid conformation, order, and dynamics by ^{2}H NMR. Biochim Biophys Acta 737:117–171

Davis JH, Bloom M, Butler KW, Smith IC (1980) The temperature dependence of molecular order and the influence of cholesterol in *Acholeplasma laidlawii* membranes. Biochim Biophys Acta 597:477–491

Epand RF, Schmitt MA, Gellman SH, Epand RM (2006) Role of membrane lipids in the mechanism of bacterial species selective toxicity by two α/β-antimicrobial peptides. Biochim Biophys Acta 1758:1343–1350

Fernandez DI, Gehman JD, Separovic F (2009) Membrane interactions of antimicrobial peptides from Australian frogs. Biochim Biophys Acta 1788:1630–1638

Fung BM, Khitrin AK, Ermolaev K (2000) An improved broadband decoupling sequence of liquid crystals and solids. J Magn Reson 142:97–101

Galassi M, Davies J, Theiler J, Gough B, Jungman G, Alken P, Booth M , Rossi F (2009) GNU Scientific Library reference manual (3rd ed vol 1.12). Network Theory Ltd. http://www.gnu.org.software/gsl/. (ISBN 0-9546120-7-8)

Guiliani A, Pirri G, Nicoletto SF (2007) Antimicrobial peptides: an overview of a promising class of therapeutics. Cent Eur J Biol 2(1):1–33

Hooper DC (2001) Mechanisms of action of antimicrobials: focus on fluoroquinolones. Clin Infect Dis 32:S9–S15

Lau T-L, Gehman JD, Wade JD, Masters CL, Barnham KJ, Separovic F (2007) Cholesterol and clioquinol modulation of Aβ (1–42) interaction with phospholipid bilayers and metals. Biochim Biophys Acta 1768:3135–3144

Mor'e JJ (1978) The Levenberg–Marquardt algorithm: implementation and theory. In: Watson G (ed) Lecture notes in Mathematics, vol 630

Oliphant CM, Green GM (2002) Quinolones: a comprehensive review. Am Fam Physician 65:455–464

Oren Z, Shai Y (1999) Mode of action of linear amphipathic α-helical antimicrobial peptides. Biopolymers (Peptide Science) 47:451–463

Park Y, Lee DG, Jang S-H, Woo E-R, Jeong HG, Choi C-H, Hahm K-S (2003) A Leu–Lys-rich antimicrobial peptide: activity and mechanism. Biochim Biophys Acta 1645:172–182

Park Y, Park SN, Park S-C, Shin SO, Kim J-Y, Kang S-J, Kim M-H, Jeong C-Y, Hahm K-S (2006) Synergism of Leu–Lys rich antimicrobial peptides and chloramphenicol against bacterial cells. Biochim Biophys Acta 1764:24–32

Sani MA, Loudet C, Grobner G, Dufourc EJ (2007) Pro-apoptotic bax-α1 synthesis and evidence for β-sheet to α-helix conformational change as triggered by negatively charged lipid membranes. J Pept Sci 13:100–106

Seelig J (1978) ^{31}P Nuclear magnetic resonance and the headgroup structure of phospholipids in membranes. Biochim Biophys Acta 515:105–140

Separovic F, Cornell B, Pace R (2000) Orientation dependence of NMR relaxation time, $T_1\rho$, in lipid bilayers. Chem Phys Lipids 107:159–167

Shai Y (1999) Mechanism of the binding insertion and destabilisation of phospholipid bilayer membranes by α-helical antimicrobial and cell non-selective membrane-lytic peptides. Biochim Biophys Acta 1462:55–70

Shai Y, Oren Z (2001) From "carpet" mechanism to de novo designed diastereomeric cell-selective antimicrobial peptides. Peptides 22:1629–1641

Shakil S, Khan R, Zarrilli R, Khan AU (2008) Aminoglycosides versus bacteria: a description of the action resistance mechanism, and nosocomial battleground. J Biomed Sci 15:5–14

Silvius JR (1982) Thermotropic phase transitions of pure lipids in model membranes and their modifications by membrane proteins lipid-protein interactions. Wiley, New York

Sreerama N, Woody RW (1993) A self-consistent method for the analysis of protein secondary structure from circular dichroism. Anal Biochem 209:32–44

Sreerama N, Woody RW (2000) Estimation of protein secondary structure from circular dichroism spectra: comparison of CONTIN, SELCON, and CDSSTR methods with an expanded reference set. Anal Biochem 287:252–260

Sreerama N, Woody RW (2004) On the analysis of membrane protein circular dichroism spectra. Protein Sci 13:100–112

Whittall KP, Sternin E, Bloom M, MacKay AL (1989) J Magn Reson 84:64–71

Yang L, Harroun TA, Weiss TM, Ding L, Huang HW (2001) Barrel-stave model or toroidal model? A case study on melittin pores. Biophys J 81:1475–1785